*Anal. Chem.* **2008,** *80,* 5203–5210

# Desorption Ionization of Biomolecules on Metals

**Nien-Yeen Hsu,[‡] Susan Yu Tseng,[†] Chung-Yi Wu,[†] Chien-Tai Ren,[†] Yuan-Chang Lee,[†] Chi-Huey Wong,[†,‡] and Chung-Hsuan Chen*[,†,‡]**

*The Genomics Research Center, Academia Sinica, Taipei, Taiwan, Republic of China, and Department of Chemistry and Chemical Biology, National Taiwan University, Taipei, Taiwan, Republic of China*

**Direct desorption ionization of various types of biomolecules on metal substrates without the need of matrices was observed by a time-of-flight mass spectrometer. It provides a new convenient method for detection of small biomolecules without the confusion of ion peaks from matrix compounds. Simple commercial Al foil can be used as the substrate to obtain mass spectra of biomolecules without the need of an etching process to produce a porous surface such as with direct ionization on silicon (DIOS). The desorption and ionization mechanism is also discussed.**



During the past 2 decades, matrix-assisted laser desorption ionization (MALDI) time-of-flight mass spectrometry has been extensively used for large-biomolecule detection. Nevertheless, MALDI is not suitable for small-biomolecule detection due to the interference of ions produced from matrix compounds. In this work, we demonstrate the direct ionization of polysaccharides, oligonucleotides, peptides, and fatty acids on metal substrates without the need of matrix.

MALDI[1,2] and electrospray ionization[3] (ESI) have been two major ionization methods for mass spectrometric analysis for large biomolecules. Due to the simplicity of the mass spectra and broad mass range, a MALDI time-of-flight mass spectrometer becomes the predominant tool for proteomic analysis without the need of preseparation by chromatography. Nevertheless, there are several disadvantages with the MALDI approach. In general, the matrix must be miscible and cocrystallize with analytes in order to get strong biomolecule signals.[4] Cocrystallization processes often produce "sweet spots" which cause poor reproducibility. In addition, the background in the low-mass region due to the matrix compound almost rules out the possibility to measure small biomolecules (<2000 Da).[5] In order to resolve this problem, various metal powders have been used for biomolecule detection.[6] Nevertheless, reproducibility was often poor and high fragmentations of biomolecules were often observed. The other approach is to immobilize matrix onto the surfaces of beads so that little matrix compound is vaporized.[7,8] This approach often involves complex processes to immobilize the matrix compound onto substrates. It is highly desirable to develop an approach for mass spectrometric analysis without the need of a matrix.

In 1999, Siuzdak and co-workers[9,10] developed desorption ionization on porous silicon (DIOS) to measure small peptides and antiviral drugs without a matrix at all. Recently, DIOS was also successfully used for the detection of a photocleavable sugar array.[11] In this approach, porous silicon was prepared by etching a silicon wafer to produce a nanostructured surface. Little background in the low-mass region was observed. Nevertheless, it is tedious to obtain reproducible surfaces with the same nanostructures. Infrared laser desorption ionization of small proteins on silicon with solvents as the matrix was also reported.[12]

Before MALDI was developed, a significant effort has been placed to study laser desorption of large organic molecules on metal substrates. In 1978, Kistemaker's group[13] reported the first successful observation of sodium-attached digoxin parent ions with the samples on a stainless steel probe. They found the mass spectra were very similar disregarding the dramatic difference in laser wavelength. Since the organic molecules used do not have any significant absorption at 1.06 $\mu$m, the ionization was attributed to the heating of the substrate instead of direct laser absorption by the large organic molecules.[13,14] In 1982, Graham et al.[15] reported laser desorption mass spectra of various cobalamins with a laser microprobe mass analyzer (LAMMA 500) with the fourth harmonics of a Nd:YAG laser with a pulse duration of 15 ns. A thermal model for the formation of alkali-attached molecular ions was also proposed by Heinen.[16] Cotter[17] found that more neutral

* To whom the correspondence should be addressed. Fax: (+882) 2-2789-9931. E-mail: winschen@gate.sinica.edu.tw.

‡ National Taiwan University.

† Academia Sinica.

(1) Karas, M.; Hillenkamp, F. *Anal. Chem.* **1988**, *60*, 2299–2301.
(2) Karas, M.; Bachmann, D.; Hillenkamp, F. *Int. J. Mass Spectrom. Ion Processes* **1987**, *78*, 53–68.
(3) Wong, S. F.; Meng, C. K.; Fenn, J. B. *J. Phys. Chem.* **1988**, *92*, 546–550.
(4) Chang, W. C.; Huang, L. C.; Wang, Y. S.; Peng, W. P.; Chang, H. C.; Hsu, N. Y.; Yang, W. B.; Chen, C. H. *Anal. Chim. Acta* **2007**, *582*, 1–9.
(5) Zhu, Y. F.; Lee, K. L.; Tang, K.; Allman, S. L.; Taranenko, N. I.; Chen, C. H. *Rapid Commun. Mass Spectrom.* **1995**, *9*, 1315–1320.
(6) Tanaka, K.; Waki, H.; Ido, Y.; Akita, S.; Yoshida, Y.; Yoshida, T. *Rapid Commun. Mass Spectrom.* **1988**, *2*, 151–153.
(7) Hutchens, T. W.; Yip, T. T. *Rapid Commun. Mass Spectrom.* **1993**, *7*, 576–580.
(8) Lin, P. O.; Tseng, M. C.; Su, A. K.; Chen, Y. J.; Lin, C. C. *Anal. Chem.* **2007**, *79*, 3401–3408.
(9) Wei, J.; Burlak, J. M.; Siuzdak, G. *Nature* **1999**, *399*, 243–245.
(10) Thomas, J. J.; Shen, Z.; Crowell, J. E.; Finn, M. G.; Siuzdak, G. *Proc. Natl. Acad. Sci. U.S.A.* **2001**, *98*, 4932–4937.
(11) Lee, J. C.; Wu, C. Y.; Apon, J. V.; Siuzdak, G.; Wong, C. H. *Angew. Chem., Int. Ed.* **2006**, *45*, 2753–2757.
(12) Bhattacharya, S. H.; Raiford, T. J.; Murray, K. K. *Anal. Chem.* **2002**, *74*, 2228.
(13) Posthumus, M. A.; Kistemaker, P. G.; Meuzelaar, H. L. C.; De Brauw, M. C. T. N. *Anal. Chem.* **1978**, *50*, 985–991.
(14) van der Peyl, G. J. Q.; Van der Zande, W. J.; Bederski, K.; Boerboom, A. J. H.; Kistemaker, P. G. *Int. J. Mass Spectrom. Ion Phys.* **1983**, *47*, 7–10.
(15) Graham, S. W.; Dowd, P.; Hercules, D. M. *Anal. Chem.* **1982**, *54*, 649–654.
(16) Heinen, H. J. *Int. J. Mass Spectrom. Ion Phys.* **1981**, *38*, 309–313.

10.1021/ac800435r CCC: $40.75 
Published on Web 05/20/2008

organic molecules were desorbed than ions. This observation is consistent with the thermal model.[17] In 1983, Kistemaker's group[18] tested the gas-phase interaction between alkali ions and gas-phase sucrose molecules and produced alkali-attached sucrose molecular ions. It indicated that alkali-attached molecular ions can be produced by ion−molecular interaction in the gas phase. A time-of-flight measurement by Hardin and Vestal[19] indicated the desorbed ion energy can reach as high as 25 eV which is outside of the range of the thermal model. Hillenkamp and co-workers[20,21] then proposed a nonthermal mechanism for desorption of ions from thin films, whereas a thermal effect is predominant in the ion evaporation from the solid. Cotter and co-workers[22–24] found the energy spread of ions formed after the laser pulse is time-dependent. In 1985, Hillenkamp's group[25] applied high-power UV laser desorption to desorb amino acids. Both tryptophan and tyrosine ions were observed. In addition, charge transfer from tryptophan to tyrosine was also observed. Tryptophan was considered as a matrix to lead to the ionization of tyrosine. This work eventually led to the discovery of MALDI.[1] After the discovery of MALDI, few reports have been focused on laser desorption ionization for mass spectrometry applications until the discovery of DIOS by Siuzdak.[9] In 1998, Owega et al.[26] reported the enhancement of ion signals with surface plasmon resonance laser desorption ionization. Yalcin et al. succeeded in the analysis of polyethylene with metal powder substrate assisted laser desorption ionization.[27] In 2007, Nayak and Knapp reported the study of laser desorption of peptides as a function of alumina pore depth and pore width.[28]

Although direct laser desorption of large molecules on metals has been actively pursued before the MALDI discovery, most results are with significantly fragmented ions. Most works were with bioorganic compound instead of regular oligonucleotides, oligosaccharides, and peptides which are the major bulk of biomolecules. In this work, we report the results of detecting oligosaccharides, peptides, and oligonucleotides without much fragmentation with laser desorption ionization on metal (DIOM). In addition, DIOM does not need a porous structure or matrix. Furthermore, we found an inexpensive commercial Al foil for cooking use can serve the purpose to measure biomolecules with DIOM. It can make routine analysis easier and less time-consuming. Since some oligosaccharides (globo-H) have been considered as potential biomarkers[29,30] for cancers and they have not been easily detected by mass spectrometry, this work can also provide a method for detecting oligosaccharide biomarkers in the future.

## EXPERIMENTAL SECTION

The mass spectrometer used to acquire the spectra was a Voyager Elite time-of-flight mass spectrometer (Applied Biosystems, Foster City, CA), equipped with a nitrogen pulsed laser (337 nm). We modified the optical path so that an external Nd:YAG laser (Laser Technik, Berlin, Germany) could also be used for laser ablation. The fourth harmonics of the Nd:YAG laser beam with wavelength at 266 nm was also used for desorption ionization of biomolecules on stainless steel. The accelerating voltage was set at 20 kV in either positive or negative ion mode. Typically, 80−100 laser shots were accumulated to obtain the final spectrum. Laser energy per pulse was calibrated with a laser power meter (PEM 101, Laser Technik, Berlin, Germany) so that laser fluence could be precisely measured. The delay extraction time could be adjusted from 10 to 500 ns. The grid voltage was set up as 95% of the accelerating voltage; the guide wire voltage was 0.2% of the accelerating voltage. The laser beam diameter was measured as ~100 $\mu$m on the sample target. The laser fluence applied was in the range of 50 to ~300 mJ/cm$^2$. The vacuum inside the flight tube was always kept between $10^{-7}$ and $10^{-6}$ Torr. Bruker's Ultraflex MALDI TOF/TOF mass spectrometer was also used to get a few mass spectra. Only the linear mode was used, and no collision-induced dissociation (CID) was pursued. Mass spectra from both instruments are very similar.

All monosaccharide, peptides, and fatty acid samples were purchased from Sigma Chemical Co. (St. Louis, MO). Oligosaccharides used in this work include mannose-1 (Man-1), mannose-4 (Man-4), mannose-7 (Man-7), and globo-H and were synthesized in our laboratory.[31,32] Synthetic oligonucleotides were purchased and synthesized with a DNA synthesizer (MDBio Inc. Taiwan). Sodium chloride (NaCl), lithium chloride (LiCl), and acetonitrile (ACN) were purchased from Merck and Co. Inc. (U.S.A.). All chemicals were of analytical grade, and doubled-distilled water was used throughout the entire work. Commercial aluminum foil (Alcoa, Richmond, VA) was used as substrate for sample deposition for mass spectrometric analysis. Other commercial Al foils from manufacturers in Taiwan were also tested with very similar results.

For most experiments, saccharide samples with the concentration of 1 nmol/$\mu$L were prepared and one drop of 1 $\mu$L was subsequently deposited onto the metal surface without matrix. Samples with aqueous sodium chloride solution or 1% trifluoroacetic acid (TFA) were also sometime incorporated into this study. The stock solution for NaCl and LiCl was prepared as 5 nmol/$\mu$L. Then an equal volume of NaCl or LiCl stock



(17) Cotter, R. J. *Anal. Chem.* **1981**, *53*, 719–720.
(18) van der Peyl, G. J. Q.; Isa, K.; Haverkamp, J.; Kistemaker, P. G. *Int. J. Mass Spectrom. Ion Phys.* **1983**, *47*, 11–14.
(19) Hardin, E. D.; Vestal, M. L. *Anal. Chem.* **1981**, *53*, 1492–1497.
(20) Hillenkamp, F. *Int. J. Mass Spectrom. Ion Phys.* **1983**, *45*, 305–307.
(21) Feigl, P.; Schueler, B.; Hillenkamp, F. *Int. J. Mass Spectrom. Ion Phys.* **1983**, *47*, 15.
(22) Cotter, R. J.; Tabet, J. C. *Int. J. Mass Spectrom. Ion Phys.* **1983**, *53*, 151–156.
(23) van Breemen, R. B.; Snow, M.; Cotter, R. J. *Int. J. Mass Spectrom. Ion Phys.* **1983**, *49*, 35–40.
(24) Tabet, J.; Cotter, R. J. *Anal. Chem.* **1984**, *56*, 1662–1667.
(25) Karas, M.; Bachman, D.; Hillenkamp, F. *Anal. Chem.* **1985**, *57*, 2935–2939.
(26) Owega, S.; Laii, E. P. C.; Bawagan, A. D. O. *Anal. Chem.* **1998**, *70*, 2360–2365.
(27) Yalcin, T.; Wallace, W. E.; Guttman, C. M.; Li, L. *Anal. Chem.* **2002**, *74*, 475–4756.
(28) Nayak, R.; Knapp, D. R. *Anal. Chem.* **2007**, *79*, 4950–4956.
(29) Wang, Z. G.; Williams, L. J.; Zhang, X. F.; Zatorski, A.; Kudryashov, V.; Ragupathi, G.; Spassova, M.; Bornmann, W.; Slovin, S. F.; Scher, H. I.; Livingston, P. O.; Lloyd, K. O.; Danishefsky, S. J. *Proc. Natl. Acad. Sci. U.S.A.* **2000**, *97*, 2719–2724.
(30) Slovin, S. F.; Ragupathi, G.; Fernandez, C.; Jefferson, M. P.; Diani, M.; Wilton, A. S.; Powell, S.; Spassova, M.; Reis, C.; Clausen, H.; Danishefsky, S.; Livingston, P.; Scher, H. I. *Vaccine* **2005**, *23*, 3114–3122.
(31) Lee, H. K.; Scanlan, C. N.; Huang, C. Y.; Calarese, D. A.; Dwek, R. A.; Rudd, P. M.; Burton, D. R.; Wilson, I. A.; Wong, C. H. *Angew. Chem., Int. Ed.* **2004**, *43*, 1000–1003.
(32) Huang, C. Y.; Thayer, D. A.; Chang, A. Y.; Best, M. D.; Hoffmann, J.; Head, S.; Wong, C. H. *Proc. Natl. Acad. Sci. U.S.A.* **2006**, *103*, 15–20.

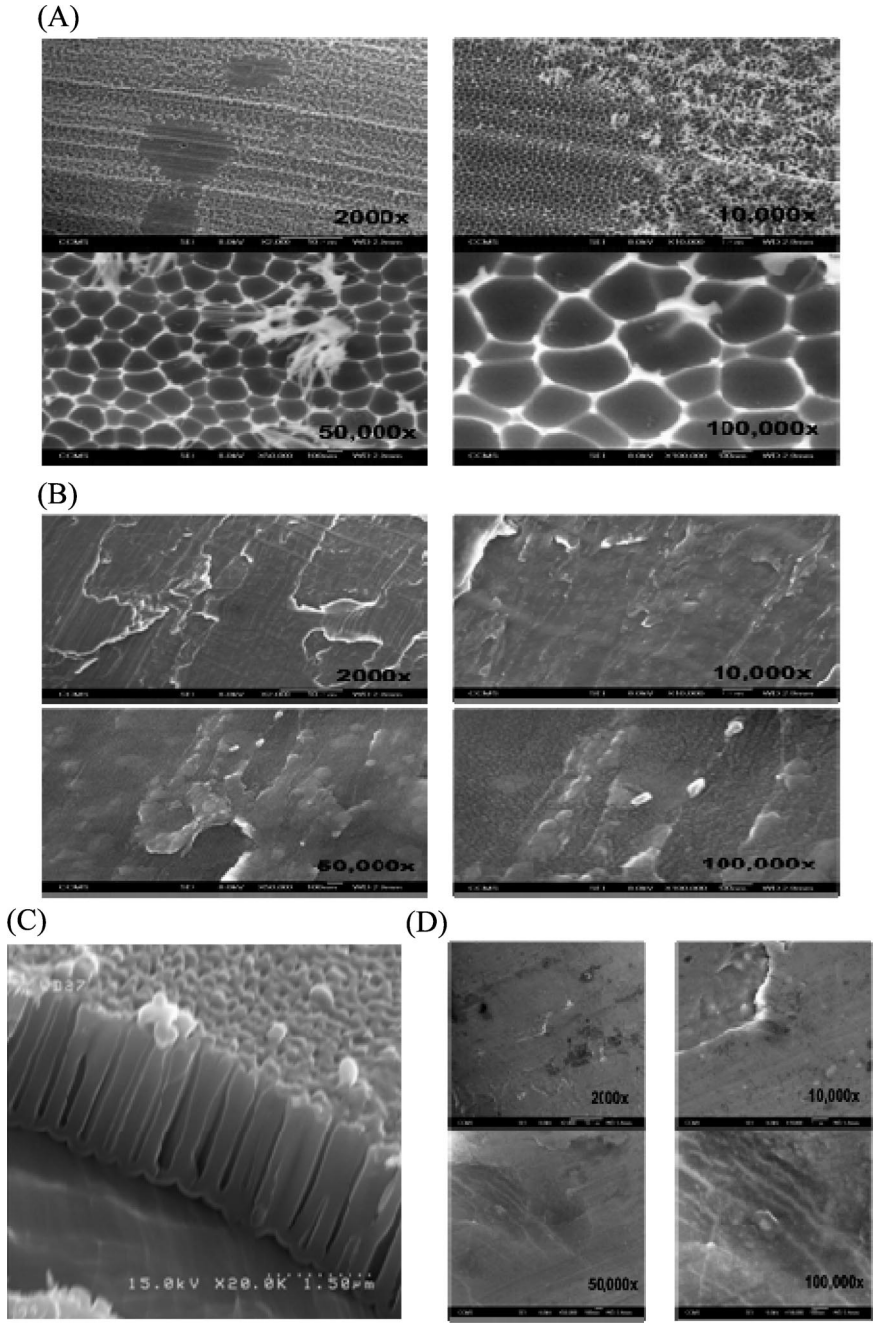




**Figure 1.** Scanning electron microscope pictures: (A) AAO pictures taken using a Joel 6700 for AAO on an aluminum plate. An aluminum plate (1 in. × 3 in. × 1 mm) was cleaned by acetone, then electropolished at 5 V (Keithley 2400 model) at room temperature in $H_3PO_4$/$H_2SO_4$/$H_2O$ (4:4:2 wt ratio) for 10 min. The anodization was conducted at 160 V, 2−5 °C in 3 M $H_3PO_4$ aqueous solution for 20 min. Then, the reaction was stopped after 20 min, and the plate was soaked in deionized water, then nitrogen purge-dried. In order to etch out the excess aluminum oxide and open up the pores, the plate was soaked in 30% $H_3PO_4$ aqueous solution for 1 h. After the etching was completed, the plate was washed again with plenty of deionized water for at least 1 h and nitrogen purge-dried. (B) NAO on an Al plate. Pictures taken using a Joel 6700 for NAO on an aluminum plate. An aluminum sheet (99.999% pure, 1 mm thick) was obtained from Nalco and cut into 1 in. × 3 in. × 1 mm sections so that it fits well into the sample holder of the mass spectrometer. The freshly cut surface of the aluminum plate has a shiny metal texture. When exposed to air, the surface gradually oxides and its appearance gradually turns opaque as a layer of aluminum oxide (called native aluminum oxide) forms. (C) Depth profile of AAO. Pictures taken using a Hitachi s4200. An aluminum sheet (99.999% pure, 0.30 mm thick) was obtained from Nalco and cut into 1 cm × 1 cm × 0.30 mm sections. The pure aluminum sheet was cleaned by acetone, dried, and electropolished at 25 V in $H_3PO_4$/$H_2SO_4$/$H_2O$ at room temperature for 10 min. The first anodization was conducted at 160 V at 2−5 °C in 0.3 M $H_3PO_4$ aqueous solution for 20 min. The reaction was stopped, and the sheet was soaked in 5% NaOH aqueous solution for 5 min to remove the alumina and to create the template. The second anodization was conducted again at the same condition. The sheet was then soaked in 0.3 M $H_3PO_4$ for 40 min to open up the pores. The thickness of the oriented AAO grown on the sheet is ∼1.5 $\mu$m. (D) The "foggy" side of Al foil. Pictures were also taken using Joel 6700 with the similar sample treatment procedure as (B). In (A), there are four image pictures from the surface of anodized aluminum oxide (AAO) with different amplification factors. Panel B includes pictures from a natural aluminum oxide (NAO) coating. Panel D includes pictures from the foggy side of commercial Al foil.

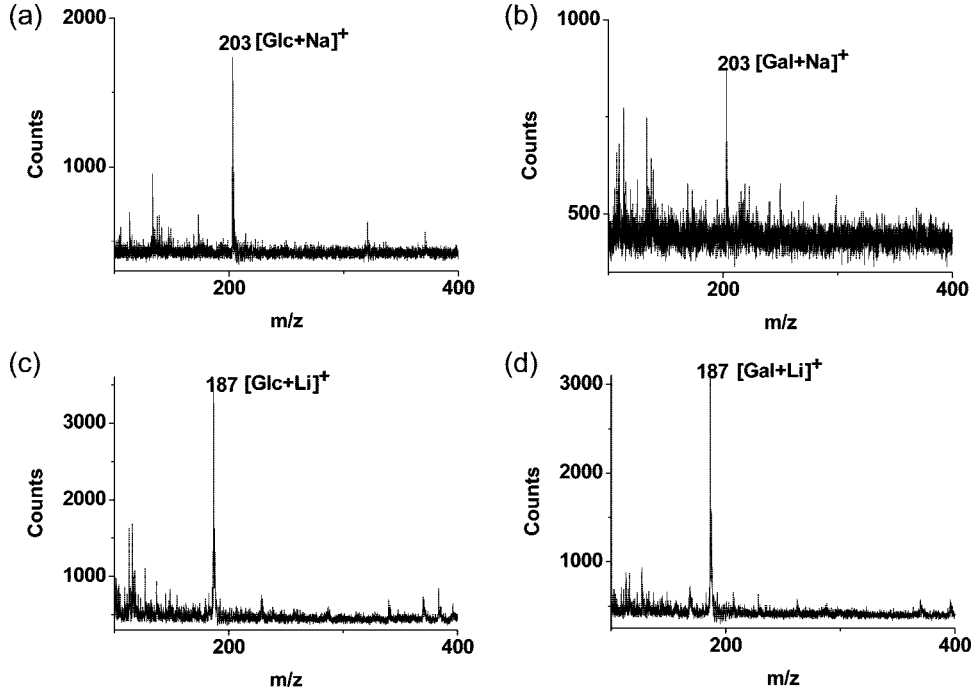


**Figure 2.** DIOM mass spectra of monosaccharides with different alkali halides on Al foils: (a) glucose; (b) galactose with NaCl on aluminum foils; (c) glucose with LiCl; (d) galactose with LiCl on aluminum foils. Glucose and galactose were used as 1 nmol/$\mu$L, NaCl and LiCl as 5 nmol/$\mu$L. Laser fluence was applied as 160 mJ/cm$^2$. Distinctive sodium and lithium adducts could be assigned.

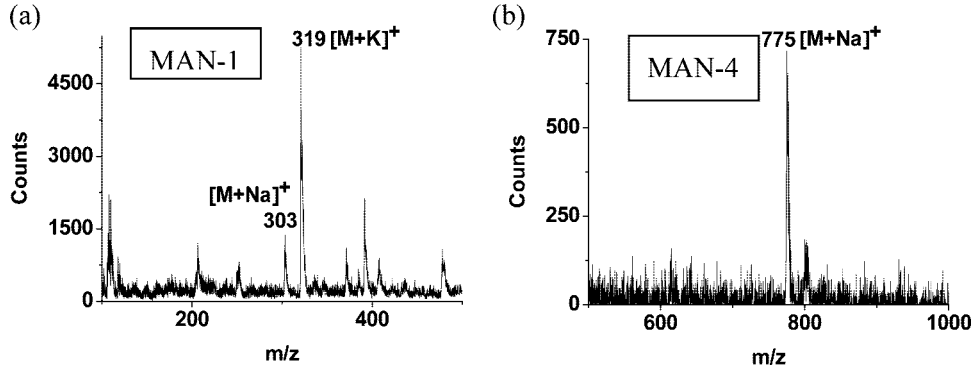


**Figure 3.** Mass spectra of (a) Man-1 and (b) Man-4 by DIOM on Al foil. Concentrations of Man-1 and Man-4 were both 100 pmol/$\mu$L. No alkali metal ions were added. Laser fluence was 200 mJ/cm$^2$. Besides the sodium ion attached adduct, a potassium-attached adduct was also observed.



solution (or 1% TFA) and saccharide solution was mixed. We typically put a 1 $\mu$L aliquot onto the metal substrate for mass spectrometry measurements.

We have used anodized aluminum oxide (AAO) and natural aluminum oxide (NAO) coating as well as commercial Al foil as substrates for direct ionization on metals. The AAO layer was grown by a typical anodization method.[33] A dc current was passed through an electrolytic solution, with the aluminum object serving as the anode. The current releases oxygen at the surface of the aluminum anode to create a buildup of aluminum oxide. NAO film was prepared with the sputtering process. Scanning electron microscopy (SEM) pictures of AAO and NAO are shown in Figure 1. SEM pictures of commercial Al foil look similar to the pictures of NAO (Figure 1D). Native aluminum oxide (NAO) grown on the aluminum surface had no orientation as compared to that of the AAO. A cross-sectional view of AAO is shown in Figure 1C.

## RESULTS AND DISCUSSION

Experimental results for monosaccharides including glucose and galactose on Al foil without any matrixes are shown in Figure 2. Different alkali salts were added to confirm the alkali atom attached ion peaks. For Figure 2, parts a and b, Na-attached ions were observed due to the addition of NaCl in the samples. For Figure 2, parts c and d, Li-attached ion peaks were observed when LiCl was added into the sample. For modified saccharides such as Man-1 and Man-4 on an Al foil, the parent ion peaks with Na attachment are clearly observed in Figure 3. Similar results were also seen for similar polysaccharides on a thin Al coating on an aluminum-coated glass slide

(33) Sheasby, P. G.; Pinner, R. The Fundamentals of Anodizing *The Surface Treatment and Finishing of Aluminum and its Alloys*, 6th ed.; ASM International & Finishing Publications: Materials Park, OH and Stevenage, U.K., 2001; Vol. 1.

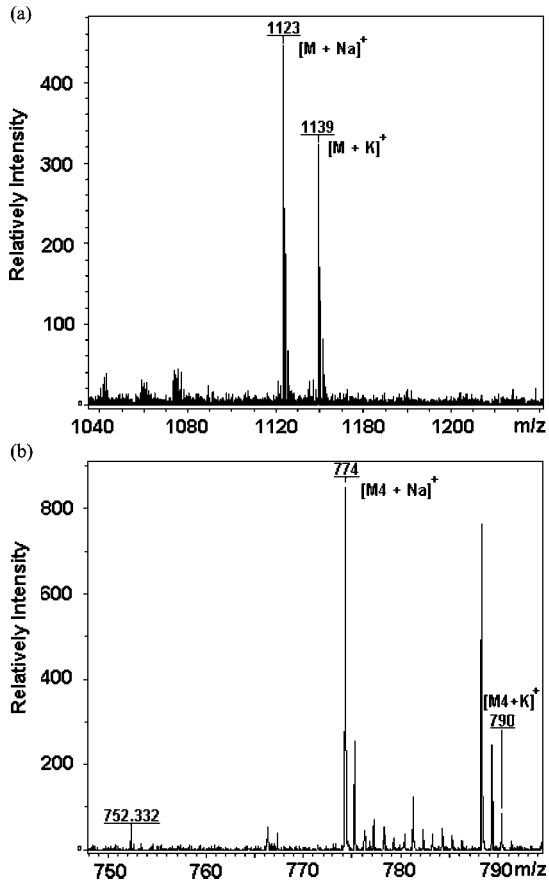


**Figure 4.** Mass spectra of (a) Man-4 and (b) globo-H of amine derivative on NAO onto aluminum oxide coated (ACG) on glass slides. NAO/ACG slide fabrication: Kimble's microglass slides (1 in. × 3 in.) and aluminum targets (99.999% pure obtained from Summit-Tech Resource Corp.) were provided by venders (Cheng-Jen Corp., Kao-Hsiung, Taiwan) for ACG slide fabrication using a magnetron sputtering coating technique. The thickness of coated aluminum on the glass slide is approximately 100 nm with 18 nm of surface roughness measured by atomic force microscopy (AFM). These ACG slides were used as is (called NAO/ACG slides). A layer of native aluminum oxide ~2−5 nm was covered on its surface. An amount of 1 $\mu$L of (a) globo-H (1.09 nmol/$\mu$L) or (b) Man-4 (6.65 nmol/$\mu$L) aqueous solution was physically deposited on the ACG slide surfaces, air-dried, and subjected for mass spectrometry analysis without the addition of the organic matrix. Peaks for protonated, Na, and K ion attached peaks are observed. However, the strong peaks with *m*/*z* at 788 and 789 could not be identified.



or on Al metal block. Experimental results of Man-4 and a globo-H derivative on an Al-coated glass surface are shown in Figure 4. In addition to the detection of saccharides, DIOM was also successfully used for the detection of fatty acids, oligonucleotide, and peptides (Figure 5). Protonated oligonucleotide was observed (Figure 5a), whereas only Na-attached ions were observed for fatty acids. Both protonated and alkali-attached signals are observed for peptides. Nevertheless, the signals of alkali-attached peptide ions are significantly stronger than the corresponding signals from protonated ions. With the limited data obtained, it appears that carbohydrates gave better mass spectra than peptides with similar mass for DIOM. Since there are no matrix compounds to provide a proton source for peptides with DIOM, it can be expected that peptides tend to have lower protonated signals. On the other hand, alkali metal always exists in any chemical and metal surface; it is easier for carbohydrates to get alkalization. It also indicates alkalization for carbohydrates is easier than alkalization of peptides (Figure 6a).

In addition to Al foil, a solid stainless steel plate was also used for DIOM. Results are shown in Figure 6. The laser beam used was a fourth harmonic of a Nd:YAG laser beam with the laser wavelength at 266 nm. For Man-1, a proton-attached ion instead of alkali ion attached peak was observed. For Man-7, three peaks with attachment of $Na^+$, $K^+$, and $Fe^+$ are observed, but few proton-attached ions were observed. The laser energy used for Man-1 was lower than that for Man-7. An alkalization signal for Man-7 was also observed on the surfaces of Al foil.

Figure 7 shows results for Man-4 by both DIOS and DIOM. It can be seen that spectrum from DIOM is simpler than that from DIOS. The signal-to-noise ratio (S/N) and mass resolution from DIOM are also better than those from DIOS. The properties of porous Si strongly depend on the etching conditions such as HF solution and etching time. The pore diameter on DIOS ranges very broad from a few nanometers to 50 nm.[34,35] The porosity is also a strong function of the preparation conditions. It can be expected that quality control for reproducibility is difficult. Since a very large amount of Al foil is produced annually with a standard procedure, it can be expected that the quality is more homogeneous. We have tried several Al foils with different manufacturers and found little difference in results. Therefore, we consider DIOM is more convenient than DIOS in term of reproducibility and the convenience to obtain the material.

The effects of surface morphology, optical absorption, and thermal conductivity in DIOS have been carefully examined by Kruse et al.[36] An internal energy transfer mechanism was recently proposed to explain the laser pulse length effect for DIOS.[37] The detailed mechanism for DIOS is still more or less unknown. Laser desorption ionization has been perceived from both nonthermal and thermal desorption.[20] A nonthermal process was speculated as the direct absorption of the sample film so that biomolecules are ejected and ionized during the laser pulse. The thermal process is from the heating of bulk which transfers energy to samples to cause desorption. This thermal emission process is slow. It can easily last at least several microseconds. Since a thermal desorption process can last microseconds or longer, the biomolecular ion peaks observed with a time-of-flight mass spectrometer in this work clearly rules out any significant contribution by a thermal desorption process. Therefore, most ions which contributed to the peaks in the mass spectra must be due to a nonthermal equilibrium process. Nevertheless, a direct absorption of a high-energy UV photon should lead to significant fragmentations which were not observed in this work.

Another puzzle of laser desorption ionization (LDI) is the source of alkali metal to form alkali metal attached ions. Alkali metal ions can exist on metal surfaces or impurities in sample preparation. Nevertheless, adding a large amount of alkali metal salts such as NaCl usually does not increase the signal of biomolecular ions. It

(34) Shen, Z. X.; Thomas, J. J.; Averbuj, C.; Broo, K. M.; Engelhard, M.; Crowell, J. E.; Finn, M. G.; Siuzdak, G. *Anal. Chem.* **2001**, *73*, 612–619.
(35) Cullis, A. G.; Canham, L. T.; Calcott, P. *J. Appl. Phys.* **1997**, *82*, 909–965.
(36) Kruse, R. A.; Li, X.; Bohn, P. W.; Sweedler, J. V. *Anal. Chem.* **2001**, *73*, 3639–3645.
(37) Luo, G.; Chen, Y.; Siuzdak, G.; Vetes, A. *J. Phys. Chem. B* **2005**, *109*, 24450–24456.

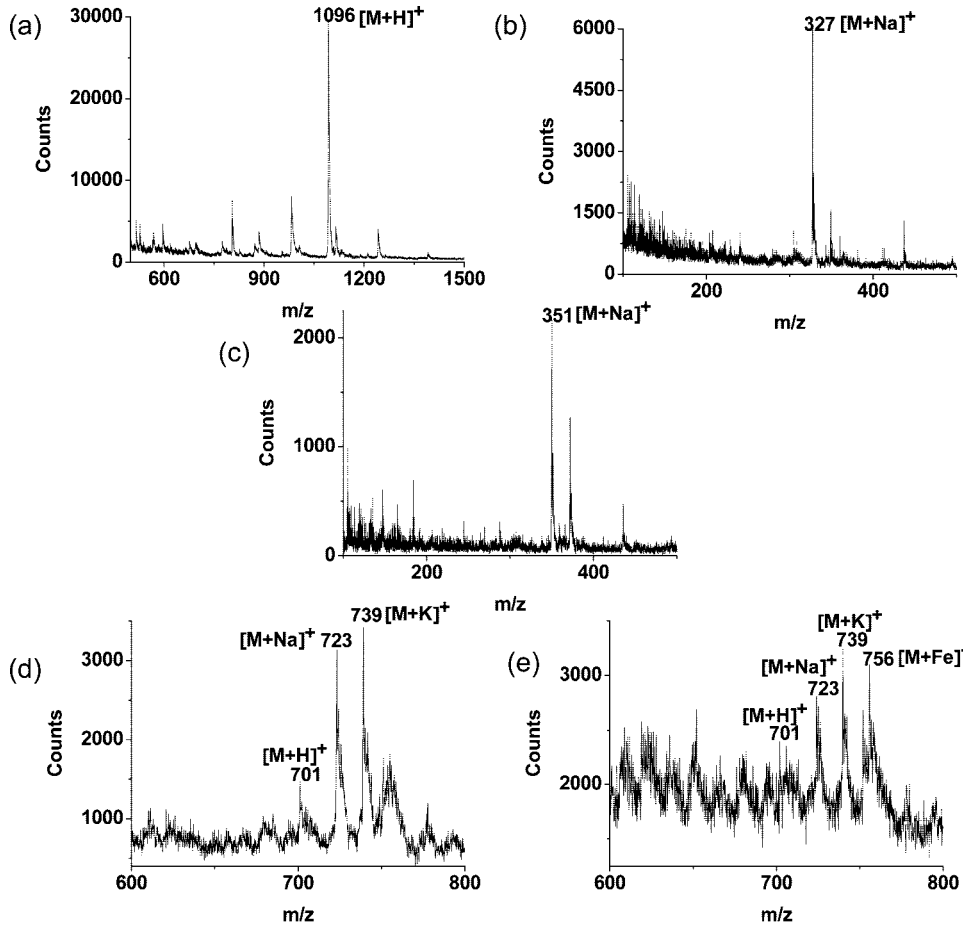


**Figure 5.** DIOM of oligonucleotide, fatty acids, and peptides: (a) oligonucleotide with sequence CCCC on Al foil; (b) arachidonic acid on Al foil; (c) *cis*-4,7,10,13,16,19-docosahexaenoic acid (DHA) on Al foil; (d) peptide (MW 700 Da) on Al foil; (e) peptide on stainless steel. The sequence of the peptide is AAAKAAAK. The concentrations of DNA, fatty acids, and peptides were 100 $\mu$M, 50 pmol/$\mu$L, and 50 pmol/$\mu$L, respectively. CCCC was dissolved with 2 mM diammonium hydrogen citrate (DAHC). Laser fluence was applied as 175, 150, and 130 mJ/cm$^2$ for DNA, fatty acids, and peptides, respectively.

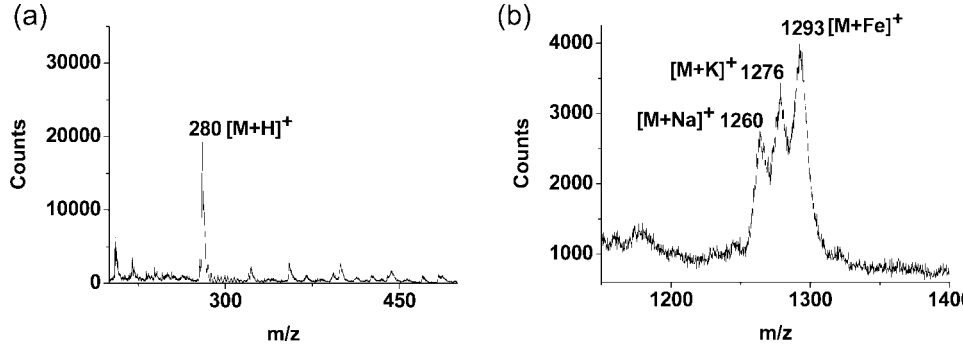


**Figure 6.** DIOM of (a) Man-1 (MW 279 Da) and (b) Man-7 (MW 1237 Da) on a stainless steel plate with Nd:YAG 266 nm laser irradiation. Laser fluence was 200 mJ/cm$^2$. The concentrations of Man-1 and Man-7 were 100 pmol/$\mu$L and 1 nmol/$\mu$L, respectively.

can rule out the formation of alkali-attached biomolecular ions being produced from collisions between biomolecules and alkali ions in the gas phase. On the other hand, the addition of NaCl or LiCl can eliminate the peaks from potassium-attached parent ions. It may indicate that alkali-attached biomolecules can be "preformed" before the LDI process. We occasionally can observe protonated saccharide ion without the signals from alkali-attached ions (Figure 6a) on the same substrate. It may also indicate the source of alkali metal is mostly from the sample.

For DIOM in this work, we like to propose a model to explain the observed phenomena. During the drying process in sample preparation, some alkali-attached pseudobiomolecular ions are formed. This mechanism can be similar to protonated or deprotonated biomolecular ions in MALDI.[38] Strong absorption of the laser beam by the substrate can cause a thermal temperature increase and a production of an acoustic wave which can lead to laser-induced acoustic desorption. Since the thermal desorption process lasts too long to get a mass spectrum with decent

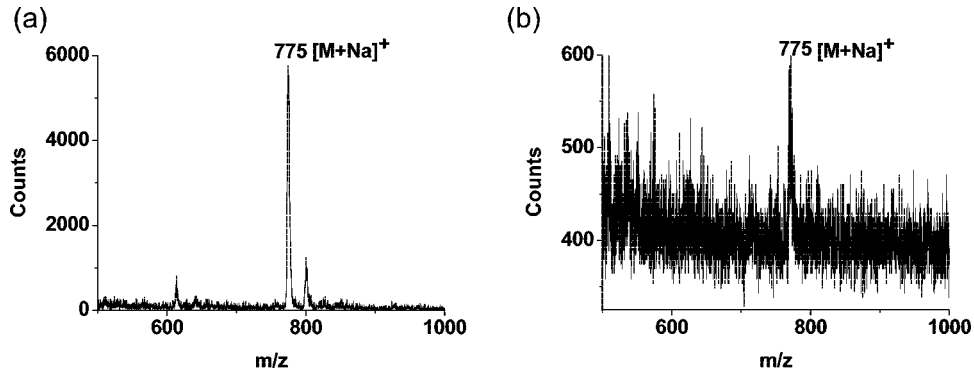


**Figure 7.** Comparison between mass spectra of Man-4 from (a) DIOM on Al foil and (b) DIOS. Laser fluence was 180 mJ/cm$^2$ in both cases. Man-4 was applied as 100 pmol/$\mu$L on each substrate. The S/N and signal intensity of DIOM are better than those of DIOS.

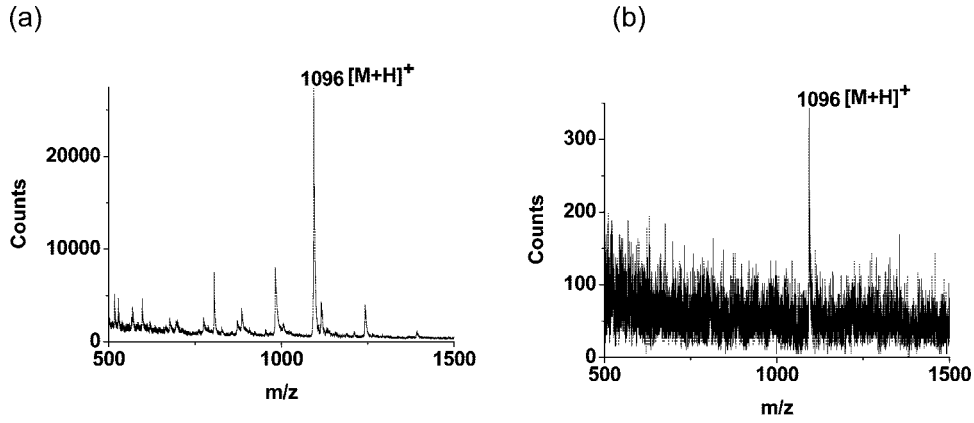


**Figure 8.** DIOM mass spectra of synthetic oligonucleotide (CCCC) from the (a) foggy and (b) bright side of Al foil. (CCCC, 100 $\mu$M dissolved with 2 mM DAHC). Laser fluence was 160 mJ/cm$^2$ on both sides. The signal intensity and S/N ratio on the Al foil foggy side show a significant difference from those on the bright side.



resolution with a time-of-flight mass spectrometer, this process can be ruled out as a major process to produce ions as discussed above. On the other hand, laser-induced acoustic desorption has been demonstrated to give efficient desorption of molecules,[39] ions,[40] nanoparticles, and cells;[41,42] it is definitely possible to have laser-induced acoustic desorption of "preformed" alkali-attached biomolecules. The other possible mechanism is multiphoton absorption of substrate to produce excitons which can transfer energy to overcome the weak interaction force between biomolecular ions and the substrate. Nevertheless, mass spectra from LDI are almost independent of laser wavelength ranging from the UV (such as the fourth harmonics of Nd:YAG at 266 nm) to the IR such as a $CO_2$ laser. These results are difficult to be explained by exciton production. On the other hand, acoustic desorption should be quite independent of laser wavelength. Ion desorption can also be achieved by field emission. It is essential to have a sharp needle structure to have efficient desorption ionization for field emission. With our AAO surface, clear needle structures can be observed by SEM (Figure 1C). Nevertheless, the amplitudes of biomolecular peaks in the mass spectra are either the same or weaker than results from samples on an aluminum foil. The possibility of field desorption to play a major role can be ruled out in LDI. Therefore, we speculate laser-induced acoustic desorption is the primary mechanism for DIOM.

We also noticed signals obtained from the "foggy" surface of Al foil are significantly higher than those from the "shining" side of Al foil (see Figure 8). In general, the "shining" side of Al foil is often coated with a thin layer of organic lubricant during the rolling process to protect the shining surface. On the other hand the "foggy" side often has no coating and is oxidized in air to produce a thin layer of aluminum oxide. Biomolecule samples were placed right on $Al_2O_3$ substrate. During the oxidation of Al in air, it is possible to have porous structures produced. High porosities can possibly be accounted for better efficiencies to obtain desorption ionization of biomolecules just like DIOS. Nevertheless, no high porosities were observed in SEM pictures (Figure 1D). For samples on the surface of the "bright" side, biomolecules actually "sit" on the organic insulator layer which is poor for electrical and thermal conductivity. Therefore, the voltage applied on the foil is less

(38) Hsu, N. Y.; Yang, W. B.; Lee, Y. C.; Lee, R. T.; Wong, C. H.; Wang, Y. S.; Chen, C. H. *Rapid Commun. Mass Spectrom.* **2007**, *21*, 2136–2147.
(39) Golovlev, V. V.; Allman, S. L.; Garrett, W. R.; Chen, C. H. *Appl. Phys. Lett.* **1997**, *71*, 852–854.
(40) Golovlev, V. V.; Allman, S. L.; Garrett, W. R.; Taranenko, N. I.; Chen, C. H. *Int. J. Mass Spectrom. Ion Processes* **1997**, *169/170*, 69–78.
(41) Peng, W. P.; Yang, Y. C.; Kang, M. W.; Tzeng, Y. K.; Nie, Z.; Chang, H. C.; Chang, W.; Chen, C. H. *Angew. Chem., Int. Ed.* **2006**, *45*, 1423–1426.
(42) Peng, W. P.; Lin, H. C.; Chu, M. L.; Yu, L. T.; Chang, H. C.; Chen, C. H. *Angew. Chem., Int. Ed.* **2007**, *46*, 3865–3869.

well-defined. The three-layer structure (Al, organics, and biomolecule sample) can also cause less efficiency to produce laser-induced acoustic desorption. Detailed mechanisms of LDI can be as complex as the MALDI mechanism and cannot be expected to be easily resolved. Our model of laser-induced acoustic desorption of preformed alkali-attached biomolecules is intended to stimulate more interest in a detailed mechanism study in the future.

In conclusion, mass spectra from DIOM are much simpler than those from MALDI due to no interference of the matrix in the low-mass region. With the success of using commercial Al foil as the substrate, DIOM can be the simplest and least expensive method to detect small biomolecules so far.

## ACKNOWLEDGMENT

This work is supported by the Genomics Research Center, Academia Sinica. Valuable suggestions and discussions with Yuan T. Lee are acknowledged.

Received for review March 3, 2008. Accepted April 16, 2008.

AC800435R